Acta Cryst E CRYSTALLOGRAPHIC COMMUNICATIONS
ISSN 2056-9890

# Crystal structure and Hirshfeld surface analysis of 2,6-diiodo-4-nitrotoluene and 2,4,6-tribromotoluene

Mohamed Larbi Medjroubi,[a]* Ali Boudjada,[a] Noudjoud Hamdouni,[a] Ouarda Brihi,[a] Olivier Jeannin[b] and Jean Meinnel[b]

[a]Laboratoire de Cristallographie, Département de Physique, Université Mentouri-Constantine, 25000 Constantine, Algeria, and [b]UMR 6226 CNRS–Université Rennes 1 'Sciences Chimiques de Rennes', Equipe 'Matière Condensée et Systèmes Electroactifs', Bâtiment 10C Campus de Beaulieu, 263 Avenue du Général Leclerc, F-35042 Rennes, France. *Correspondence e-mail: medjroubi-m@umc.edu.dz

Received 16 June 2020
Accepted 23 July 2020

Edited by G. Diaz de Delgado, Universidad de Los Andes, Venezuela

**Keywords:** X-ray diffraction; crystal structure; 2,6-diiodo-4-nitrotoluene; 2,4,6-tribromotoluene; Hirshfeld surface.

**CCDC references**: 2018692; 2018691

**Supporting information**: this article has supporting information at journals.iucr.org/e

The title compounds, 2,6-diiodo-4-nitrotoluene (DINT, $C_7H_5I_2NO_2$) and 2,4,6-tribromotoluene (TBT, $C_7H_5Br_3$,), are trisubstituted toluene molecules. Both molecules are planar, only the H atoms of the methyl group, and the nitro group in DINT, deviate significantly from the plane of the benzene ring. In the crystals of both compounds, molecules stack in columns up the shortest crystallographic axis, *viz*. the *a* axis in DINT and the *b* axis in TBT. In the crystal of DINT, molecules are linked *via* short N—O···I contacts, forming chains along [100]. In TBT, molecules are linked by C—H···Br hydrogen bonds, forming chains along [010]. Hirshfeld surface analysis was used to explore the intermolecular contacts in the crystals of both DINT and TBT.

## 1. Chemical context

In order to understand the methyl radical behaviour of benzene molecules substituted by halogens and methyl groups, we have studied a number of halogenomesitylenes, such as triiodomesitylene (TIM; Boudjada *et al.*, 2001), trichloromesitylene (TCM; Tazi *et al.*, 1995), tribromomesitylene (TBM; Boudjada *et al.*, 1999) and dibromomesitylene (DBM; Hernandez *et al.*, 2003). In the solid state of these halogenomethyl-benzene (HMB) compounds, the steric hindrance between the methyl group and the halogen atoms results in small out-of -plane deformations of the heavy atoms. In spite of the small amplitudes of the deformation, the impact on the rotational potential of the methyl group is considerable because of the contribution of the neighbouring halogen atoms on the methyl groups as observed in these planar structures. This study has now been extended to understand and identify the methyl-group behaviour of halogeno-toluene molecules, and we report herein on the crystal and molecular structures of the title compounds, 2,6-diiodo-4-nitrotoluene (DINT; systematic name: 1,3-diiodo-2-methyl-5-nitrobenzene) and 2,4,6-tribromotoluene (TBT; systematic name: 1,3,5-tribromo-2-methyl-benzene). Hirshfeld surface analysis was used to explore the intermolecular contacts in the crystals of both compounds.

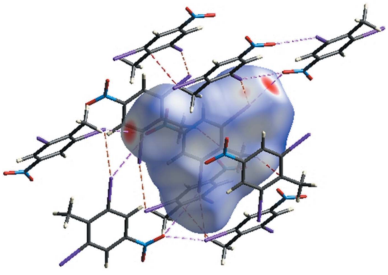

## 2. Structural commentary

The molecular structure of DINT is illustrated in Fig. 1, and that of TBT in Fig. 2. The structures of the title compounds are

compared with those of the dichloronitrotoluene (DCNT; Medjroubi *et al.*, 2017) and dibromonitrotoluene (DBNT; Medjroubi *et al.*, 2016) analogues, illustrated in Fig. 3.

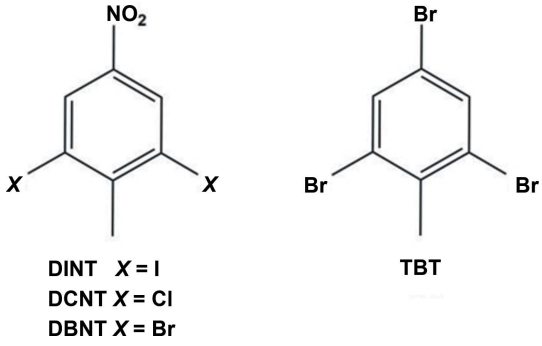


In DBNT, the methyl group exhibits rotational disorder about the $C_{ar}-C_{me}$ axis. As in DCNT, the methyl group of DINT does not present any disorder. Hence, no significant steric hindrance of the methyl group by the *ortho* halogen atoms is observed. The longest bond lengths $C_{ar}-C_{ar}$ are adjacent to the $C_{ar}-C_{me}$ bond with an average value of 1.405 (4) Å. The bond-length values are close to those found in the literature. Moreover, in the crystal structure of DINT, the methyl group has a C—H bond perpendicular to the mean plane with a torsion angle C2—C1—C7—H7*A* = 90.0°, which has already previously been reported in the literature. The intermolecular N1—O···I [3.115 (3) Å] interactions are competing to ensure cohesion in the crystal, see Fig. 4. Atom I2 bonded to the atom C6, with the C1—C6—I2 angle of 121.7 (3)° being greater than the angle C5—C6—I2 [116.1 (2)°] located on the other side of the C6—I2 bond (Fig. 1). The aromatic ring is planar in DINT. The methyl C atom, the I atoms and the N atom of the nitro substituent, lie extremely close to the plane of the benzene ring; the deviations are 0.001 (1) Å for the methyl C atom, 0.097 (3) and −0.097 (3) Å for the two I atoms, −0.011 (2) Å for the nitro N atom, whereas for the oxygen atoms, which are located on either side of the mean plane, the deviations are 0.293 (3) and −0.283 (3) Å. In the crystal of DCNT, molecules are linked by weak C—H···O and C—H···Cl hydrogen bonds, forming layers parallel to the *ab* plane Fig. 5 (Medjroubi *et al.*, 2017).

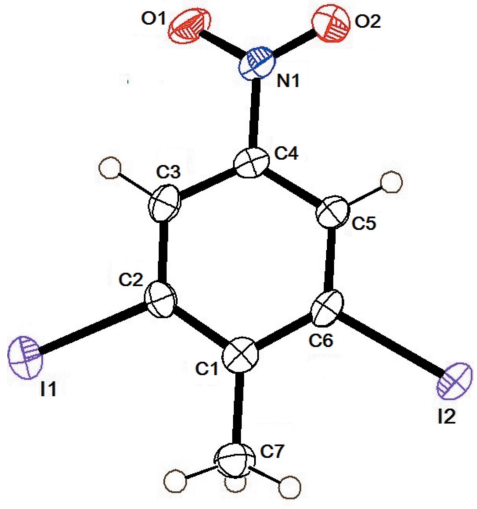


**Figure 1**
The molecular structure of DINT with the atom labelling and displacement ellipsoids drawn at the 50% probability level.

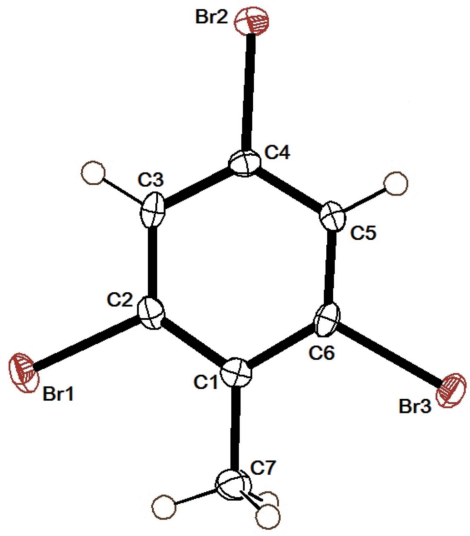


**Figure 2**
The molecular structure of TBT with the atom labelling and displacement ellipsoids drawn at the 50% probability level.

The molecular structure of TBT is illustrated in Fig. 2. The structural study did not reveal any disorder and the intramolecular interaction ensuring the cohesion in the crystal is C—Br··· H7*B* (2.61 Å) as seen in Fig. 6 and Table 1. This

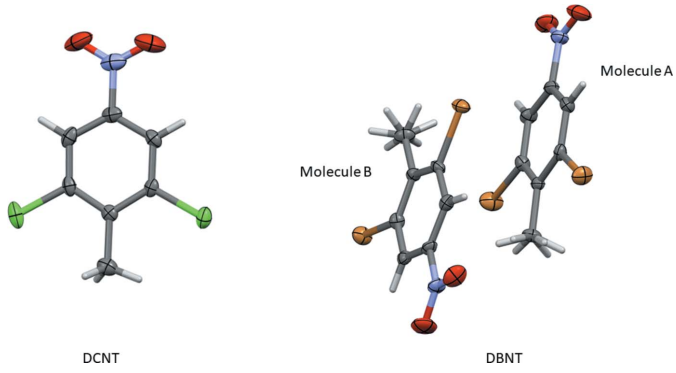


**Figure 3**
The molecular structures of DCNT and DBNT, with displacement ellipsoids drawn at the 50% probability level.

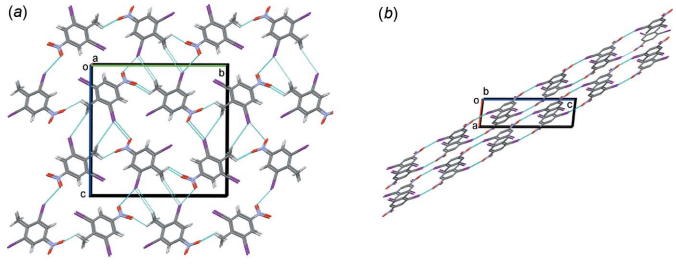


**Figure 4**
A view along the *a* and *b* axes of the crystal packing of DINT.

**Table 1**
Hydrogen bonds (Å, °) for (I) and (II).

| Compound | $D$—H···$A$ | $D$—H | H···$A$ | $D$···$A$ | $D$—H···$A$ |
|---|---|---|---|---|---|
| (I) | C7—H7$B$···I1 | 0.98 | 2.82 | 3.333 (4) | 113 |
| | C7—H7$C$···I2 | 0.98 | 2.84 | 3.331 (4) | 112 |
| (II) | C7—H7$B$···Br1 | 0.98 | 2.61 | 3.199 (3) | 118 |

conformation produces a significant steric effect between the hydrogen atoms of the methyl group and atom Br2 bonded to atom C6 with an angle C1—C6—Br3 = 119.8 (2)°, which is clearly greater than the angle C5—C6—Br3 = 116.5 (2)° located on the other side of the C6—Br1 bond. This is the same case for the exocyclic angles C6—C1—C7 = 121.9 (3)° and C2—C1—C7 = 123.6 (3)° located on either side of the C1—C7 bond. As found in DINT and DCNT, the longest $C_{ar}$—$C_{ar}$ bond lengths are adjacent to the $C_{ar}$–$C_{me}$ bond (Fig. 2). The methyl C atom C7 is displaced from the benzene ring by −0.005 (1) Å, while the Br atoms lie almost in the plane of the benzene ring [deviations are 0.003 (3) Å for atoms Br1 and Br3 and −0.012 (3) Å for atom Br2]. The $CH_3$ group presents an eclipsed C—H bond with the mean plane of the molecule. A difference of 2° is found between the exocyclic angles $C_{ar}$—$C_{ar}$—$C_{me}$, which explains the importance of the interaction of this eclipsed bond with atom Br3. The endocyclic angle in front of the methyl group is equal to 116.6 (3)° for DINT, 115.7 (2)° for DCNT (Medjroubi *et al.*, 2017), 114.7 (3)° for DBNT (Medjroubi *et al.*, 2016) and 114.5 (3)° for TBT. The variation of this angle is very sensitive to the substitution of the halogen atoms surrounding the methyl groups of these different compounds.

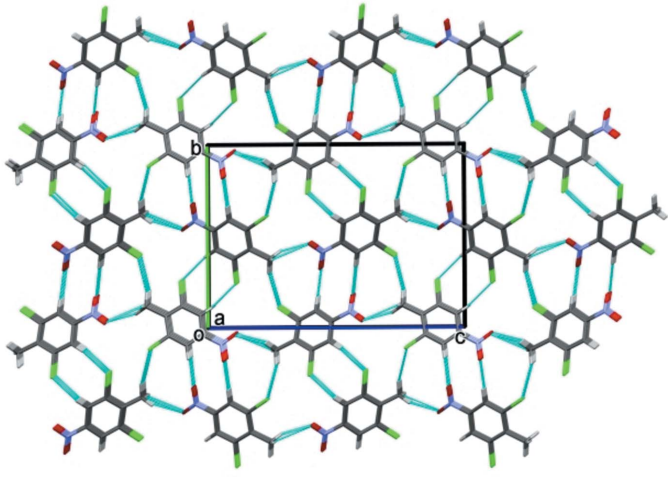


**Figure 5**
A view along the *a* axes of the crystal packing of 2,6-dichloro-4-nitrotoluene, DCNT.

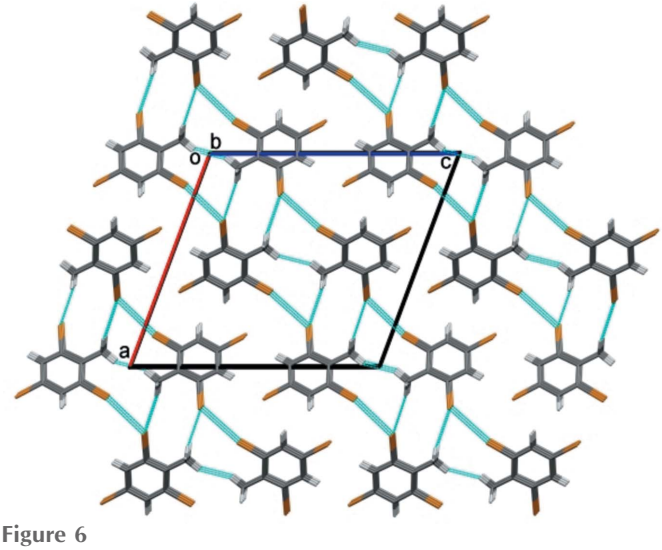


**Figure 6**
A view along the *b* axes of the crystal packing of 2,4,6-tribromotoluene, DBNT.

**Table 2**
Short contacts and contributions (%) to the Hirshfeld surface for DINT, DCNT and TBT.

| DINT | | DCNT | | TBT | |
|---|---|---|---|---|---|
| Contact | % | Contact | % | Contact | % |
| I···H/H···I | 25.7 | Cl···H/H···Cl | 26.8 | Br···H/H···Br | 42.7 |
| I···O/O···I | 16.0 | | | | |
| O···H/H···O | 15.6 | O···H/H···O | 26.1 | | |
| H···H | 12.7 | H···H | 9.1 | H···H | 18.2 |
| C···H/H···C | 11.1 | C···H/H···C | 6.9 | C···H/H···C | 8.0 |
| O···C/C···O | 5.3 | | | | |
| I···I | 4.8 | Cl···Cl | 5.9 | Br···Br | 17.4 |
| C···C | 3.4 | C···C | 7.4 | C···C | 7.3 |
| | | Cl···O/O···Cl | 5.0 | | |
| | | Cl···C/C···Cl | 5.1 | Br···C/C···Br | 6.4 |

## 3. Supramolecular features

In the crystal of DINT, the molecules are assembled into columns along the *a*-axis direction, the shortest crystallographic axis. Molecules are linked by O···I intermolecular interactions, with distance I2···O1$^{i}$ = 3.12 (1) Å [symmetry code (i): $x-1, -y+\frac{1}{2}, z+\frac{1}{2}$], leading to the formation of chains along the [20$\overline{1}$] direction, see Fig. 4.

In the crystal of TBT, molecules stack in columns along the *b*-axis direction, again the shortest crystallographic axis. Molecules are linked by weak Br···Br interactions [Br1···Br3$^{ii}$ = 3.5921 (5) Å; symmetry code (ii): $x+\frac{1}{2}, -y+\frac{3}{2}, z+\frac{1}{2}$], forming chains along the [101] direction. Br···H short contacts are also present in the crystal of TBT [Br1···H7$C^{ii}$ = 3.5921 (5) Å; symmetry code (iii): $x, -1+y, z$].

## 4. Analysis of the Hirshfeld surfaces of DINT and TBT

Additional insight into the intermolecular interactions was obtained from analysis of the Hirshfeld surface (HS) (Spackman & Jayatilaka, 2009) and the two-dimensional fingerprint plots (McKinnon *et al.*, 2007). The program *CrystalExplorer* (Turner *et al.*, 2017) was used to generate Hirshfeld surfaces mapped over $d_{norm}$ and the electrostatic potential for compounds TBT and DINT. The function $d_{norm}$ is a ratio enclosing the distances of any surface point to the nearest interior ($d_i$) and exterior ($d_e$) atom and the van der Waals (vdW) radii of the atoms. The electrostatic potentials were

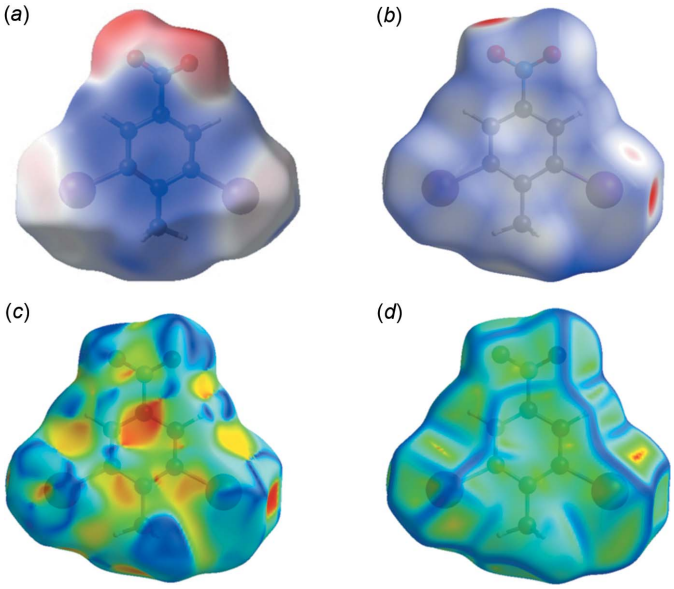


**Figure 7**
Hirshfeld surface for DINT mapped over (*a*) calculated electrostatic potential, (*b*) $d_{norm}$, (*c*) shape-index and (*d*) curvedness.

calculated using *TONTO* (Spackman & Jayatilaka, 2009) integrated into *CrystalExplorer*, using the crystal structure as the starting geometry. Short contacts and contributions to the Hirshfeld surface for DINT, DCNT (Medjroubi *et al.*, 2017) and TBT are given in Table 2. The Hirshfeld surface (HS) mapped over the electrostatic potential for DINT in the range [−0.071 to +0.041], is shown in Fig. 7*a* where the red and blue regions represent negative and positive electrostatic potentials respectively. The Hirshfeld surface mapped over $d_{norm}$ is depicted in Fig. 7*b*. The HS mapped over shape-index and curvedness are shown in Fig. 7*c* and 7*d*, respectively.

The crystal environment about a DINT molecule is illustrated in Fig. 8: the interactions are shown on the Hirshfeld surfaces with short contacts indicated in red. The two-dimensional fingerprint plots for all contacts are illustrated in Fig. 9*a*. The I···O/O···I interaction ensures the cohesion of

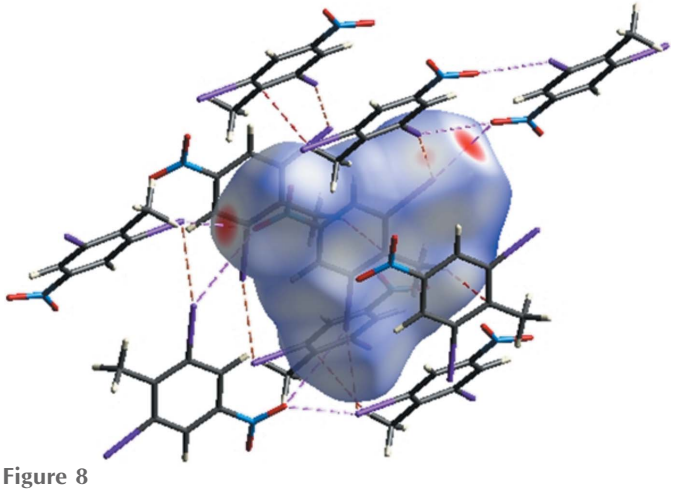

**Figure 8**
A view of the Hirshfeld surface of DINT mapped over $d_{norm}$, with interactions shown as dashed lines.

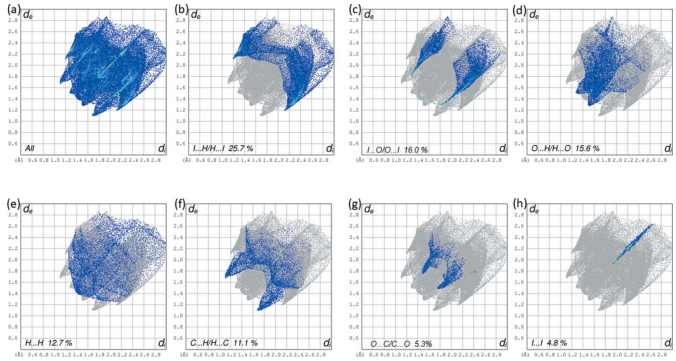


**Figure 9**
(*a*) The full two-dimensional fingerprint plot calculated for DINT and those delineated into (*b*) I···H/H···I contacts, (*c*) I···O/O···I contacts, (*d*) O···H/H···O contacts, (*e*) H···H contacts, (*f*) C···H/H···C contacts, (*g*) O···C/C···O contacts and (*h*) I···I contacts.

the crystal with a contribution of 16% of all the interactions appearing in bright-red spots on the Hirshfeld surfaces mapped over $d_{norm}$. The fingerprint consists of two spikes with the ends at $d_e + d_i \simeq 3.1$ Å, Fig. 9*c*. The fingerprint of the C···H/H···C interaction consists of two symmetrical peaks with a $d_e + d_i \simeq 2.8$ Å, Fig. 9*f* and almost equal to the sum of van der Waals radii. It is represented on the HS mapped with the shape-index property in the form of a pale-red spot, Fig. 7*c*. The I···I interaction is less important than O···I/I···O; however, it does contribute 4.8% to the total interactions, illustrating the equality of the I···I distance to the sum of van der Waals radii. The fingerprint is composed of a single peak in the form of a needle with $d_e + d_i \simeq 3.8$ Å, Fig. 9*h*. The absence of $\pi$–$\pi$ stacking interactions is consistent with the low contributions of C···C contacts to the Hirshfeld surface (Table 2). The Hirshfeld surface analysis (Fig. 10*b*) and elec-

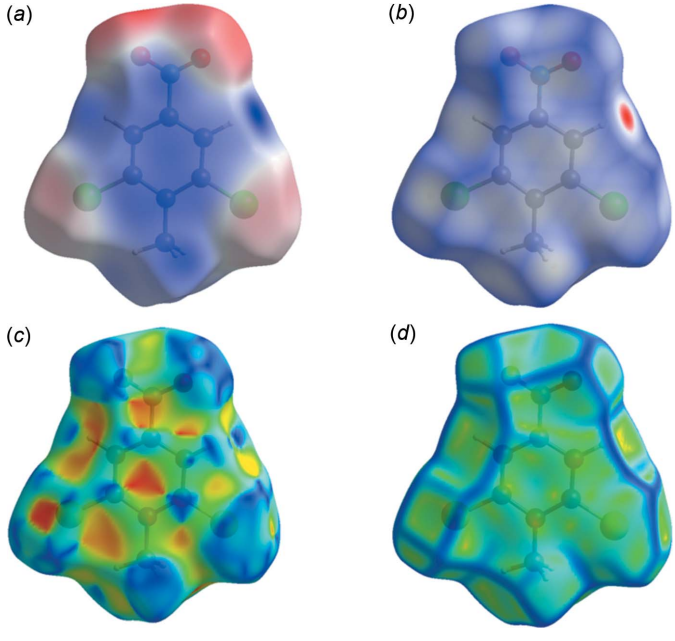


**Figure 10**
Hirshfeld surface for DCNT mapped over (*a*) calculated electrostatic potential, (*b*) $d_{norm}$, (*c*) shape-index and (*d*) curvedness.

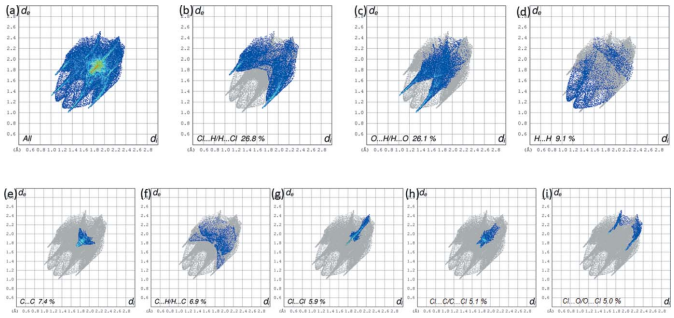

Figure 11
(*a*) The full two-dimensional fingerprint plot calculated for DCNT and those delineated into (*b*) Cl···H/H···Cl contacts, (*c*) O···H/H···O contacts, (*d*) H···H contacts, (*e*) C···C contacts, (*f*) C···H/H···C contacts, (*g*) Cl···Cl contacts, (*h*) Cl···C/C···Cl contacts and (*i*) Cl···O/O···Cl contacts.

trostatic potential surface (Fig. 10*a*) show the intermolecular interactions between different units in the crystalline environment of DCNT. The HS mapped over shape-index and curvedness are shown in Fig. 10*c* and *d*, respectively. The two-dimensional fingerprint plots for all contacts are illustrated in Fig. 11. The contributions of the major intermolecular contacts in the title compound are Cl···H/H···Cl (26.8%), O···H/H···O (26.1%), and H···H (10.6%) (Fig. 11*a*). Other contacts (*e.g.* C···C, H···C/C···H, Cl···Cl, Cl···C/C···Cl, Cl···O/O···Cl) make contributions of less than 7.5% to the HS. The graph shown in Fig. 11*b* represents the one-third of all the intermolecular contacts. All fingerprint points are located at distances with $d_i$ equal to or greater than van der Waals distances, $d_e + d_i \simeq 1.27$ Å, reflecting a zero tendency to form this intermolecular contact (Cl···H). The graph shown in Fig. 11*c* (O···H/H···O) shows the contact between the

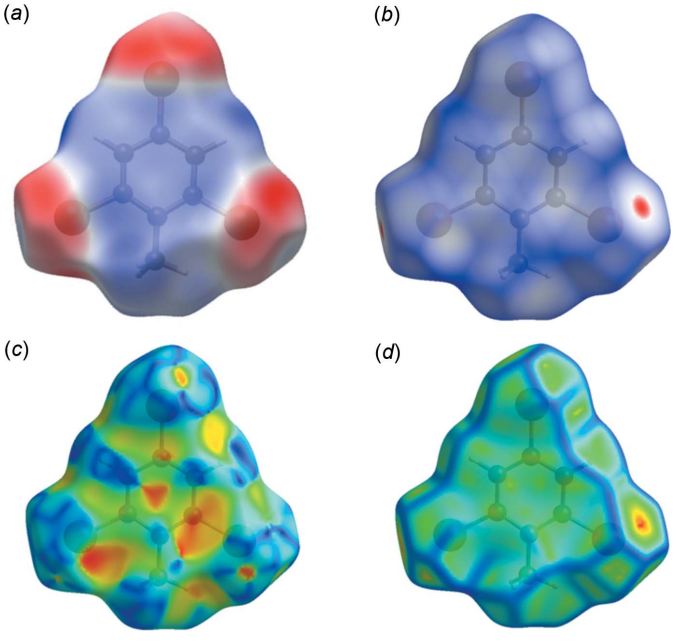

Figure 12
Hirshfeld surface for TBT mapped over (*a*) calculated electrostatic potential, (*b*) $d_{norm}$, (*c*) shape-index and (*d*) curvedness.

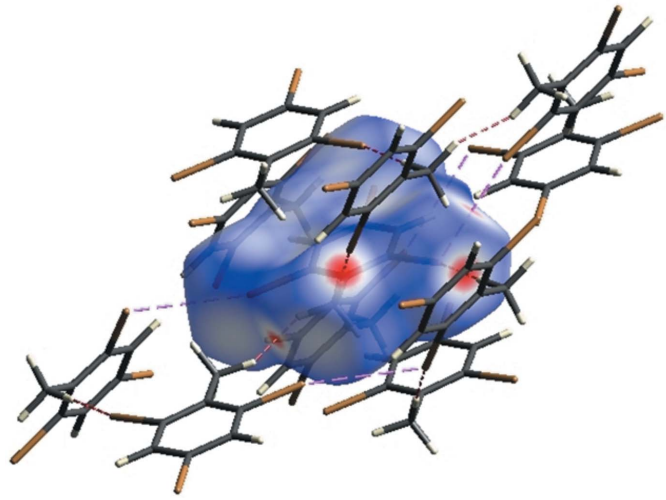

Figure 13
A view of the Hirshfeld surface of TBT mapped over $d_{norm}$, with interactions shown as dashed lines.

oxygen atoms inside the surface and the hydrogen atoms outside the surface, $d_e + d_i \simeq 2.35$ Å, and has two symmetrical points at the top, bottom left and right. The graph shown in Fig. 11*d* (H···H; 10.6%) shows the two-dimensional fingerprint of the ($d_i$, $d_e$) points associated with hydrogen atoms, which has two symmetrical wings on the left and right with $d_e + d_i \simeq 2.3$ Å.

The electrostatic potentials were mapped on the Hirshfeld surface using the STO-3G basis/Hartree–Fock level of theory over the range [−0.016, 0.036] for TBT (Fig. 12). Atoms H7*A*, H7*B* and H7*C* of the methyl group and H3, H5 as donors, and the bromine atom acceptors, are also evident in Fig. 12*a*. The Hirshfeld surface mapped over $d_{norm}$ is depicted in Fig. 12*b*. The overall 2D fingerprint plot is presented in Fig. 13*a*. The halogen–halogen (Br···Br) interaction contributes 17.4% to the HS and ensures the cohesion of the crystal and dictates the intermolecular stacking. The short intramolecular H···Br/Br···H contact between C3—H7*B* and Br1 (H7*B*···Br1 = 2.6 Å) can be recognized from the two neighbouring blue

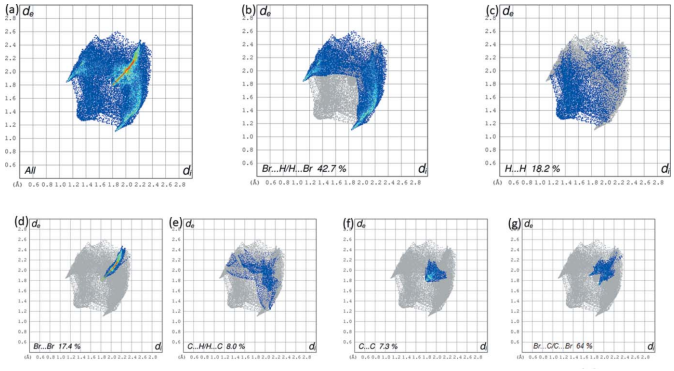

Figure 14
(*a*) The full two-dimensional fingerprint plot calculated for TBT and those delineated into (*b*) Br···H/H···Br contacts, (*c*) H···H contacts, (*d*) Br···Br contacts, (*e*) C···H/H···C contacts, (*f*) C···C contacts and (*g*) Br···C/C···Br contacts.

Table 3
Experimental details.

| | DINT | TBT |
|---|---|---|
| Crystal data | | |
| Chemical formula | $C_7H_5I_2NO_2$ | $C_7H_5Br_3$ |
| $M_r$ | 388.92 | 328.84 |
| Crystal system, space group | Monoclinic, $P2_1/c$ | Monoclinic, $P2_1/n$ |
| Temperature (K) | 150 | 150 |
| $a, b, c$ (Å) | 4.3815 (2), 15.3348 (6), 14.5894 (6) | 14.3484 (11), 3.9955 (3), 15.6975 (12) |
| $\beta$ (°) | 96.588 (1) | 110.519 (2) |
| $V$ (Å$^3$) | 973.78 (7) | 842.83 (11) |
| $Z$ | 4 | 4 |
| Radiation type | Mo $K\alpha$ | Mo $K\alpha$ |
| $\mu$ (mm$^{-1}$) | 6.42 | 14.28 |
| Crystal size (mm) | 0.29 × 0.13 × 0.06 | 0.34 × 0.21 × 0.12 |
| Data collection | | |
| Diffractometer | Bruker APEXII | Bruker APEXII |
| Absorption correction | Multi-scan (*SADABS*; Bruker, 2006) | Multi-scan (*SADABS*; Bruker, 2006) |
| $T_{min}$, $T_{max}$ | 0.382, 0.680 | 0.496, 0.746 |
| No. of measured, independent and observed [$I > 2\sigma(I)$] reflections | 4104, 2244, 1850 | 6197, 1928, 1657 |
| $R_{int}$ | 0.022 | 0.027 |
| (sin $\theta/\lambda)_{max}$ (Å$^{-1}$) | 0.651 | 0.650 |
| Refinement | | |
| $R[F^2 > 2\sigma(F^2)]$, $wR(F^2)$, $S$ | 0.024, 0.046, 0.98 | 0.025, 0.049, 1.08 |
| No. of reflections | 2244 | 1928 |
| No. of parameters | 110 | 93 |
| H-atom treatment | H-atom parameters constrained | H-atom parameters constrained |
| $\Delta\rho_{max}$, $\Delta\rho_{min}$ (e Å$^{-3}$) | 0.65, −0.55 | 0.70, −0.68 |

Computer programs: *APEX2* and *SAINT* (Bruker, 2006), *SIR2004* (Burla *et al.*, 2005), *SHELXL2018/3* (Sheldrick, 2015), *ORTEP-3 for Windows* and *WinGX* publication routines (Farrugia, 2012) and *Mercury* (Macrae *et al.*, 2020).

regions on the surface mapped with electrostatic potential in Fig. 14*c*,*d*. The two-dimensional fingerprint plot delineated into Br···H/H···Br has two peaks pointing to the pairs $d_e + d_i \simeq 3.0$ Å, slightly lower than or equal to the sum of van der Waals radii, Fig. 14*b*. These correspond to a 42.7% contribution to the Hirshfeld surface, and reflect the presence of intermolecular C7—H7*C*···Br3 interactions. The interatomic H···H contacts at distances greater than their van der Waals separation appear as scattered points in the greater part of the fingerprint plot Fig. 14*c*. The presence of C—H···$\pi$ and H—C···$\pi$ stacking interactions between the TBT rings is also apparent from the appearance of red and blue triangle pairs on the Hirshfeld surface mapped with shape-index property identified with arrows in Fig. 12*c*. The immediate environment about each molecule highlighting close contacts to the Hirshfeld surface by neighboring molecules is shown in Fig. 13. The relative contributions to the overall surface are given in Table 2.

## 5. Database survey

A search of the Cambridge Structural Database (CSD, Version 5.40, last update May 2019; Groom *et al.*, 2016) for 2,6-diiodo-4-nitrotoluene (DINT) and 2,4,6-tribromotoluene (TBT) gave five hits: 2,6-dichloro-4-nitrotoluene (DCNT; Medjroubi *et al.*, 2017), dibromonitrotoluene (DBNT; Medjroubi *et al.*, 2016), triiodomesitylene (TIM) (Boudjada *et al.*, 2001), tribromomesitylene (TBM; Boudjada *et al.*, 1999) and dibromomesitylene (DBM; Hernandez *et al.*, 2003). In DBNT (Medjroubi *et al.*, 2016), there are two independent molecules per asymmetric unit and the methyl group H atoms are positionally disordered, as found for DBM (Hernandez *et al.*, 2003). While in the compounds DINT and DCNT (Medjroubi *et al.*, 2017), there is only one molecule in the asymmetric unit and no disorder is observed for the methyl group H atoms. In the molecule of DINT, a $C_m$—H (m = methyl) bond is perpendicular to the mean plane of the molecule, as found for triiodomesitylene (TIM; Boudjada *et al.*, 2001). The nitro group is inclined to the benzene ring by 16.72 (1)° in DINT, compared with 9.8 (3)° in DCNT, and 2.5 (5)° and 5.9 (4)° in DBNT. In the molecule of TBT, the $CH_3$ group presents an eclipsed C—H bond with the mean plane of the molecule. This also applies to DCNT (Medjroubi *et al.*, 2017), which does not present any disorder, as was also found in the case of tribromomesitylene TBM (Boudjada *et al.*, 1999). In 2,6-dihalogeno-4-nitrotoluene, as in the title compounds, the cohesion of the crystal is ensured by interactions of the type C—H···halogen and C—halogen···halogen.

## 6. Synthesis and crystallization

**2,6-Diiodo-4-nitrotoluene (DINT):** 4-nitrotoluene (0.68g, 5 mmol) was suspended in 90% (*v*/*v*) conc. $H_2SO_4$ (10 ml) at 298–303 K. While keeping the same temperature, the iodinating solution containing the $I^+$ intermediate in *ca* 50% excess was added dropwise under stirring over 45 min. The stirring was continued at 298–303 K for a further 75 min. The final reaction mixture was poured, with stirring, into ice–water

(300 g). The crude solid obtained was recrystallized from ethanol (27 ml). On slow evaporation of the solvent, colourless prismatic crystals of DINT were obtained (yield 77%, 1.5 g).

**2,4,6-Tribromotoluene (TBT)** is commercially available (Sigma–Aldrich). It was recrystallized from ethanol solution, giving large colourless needle-like crystals, many of which were twinned.

## 7. Refinement details

Crystal data, data collection and structure refinement details for DINT and TBT are summarized in Table 3. The H atoms were included in calculated positions and refined as riding: C—H = 0.95–0.98 Å with $U_{iso}$(H) = 1.5$U_{eq}$(C-methyl) and 1.2$U_{eq}$(C) for other H atoms.

## Acknowledgements

We would like to thank the Centre de Diffractométrie de l'Université de Rennes 1 for the data collection.

## References

Boudjada, A., Hernandez, O., Meinnel, J., Mani, M. & Paulus, W. (2001). *Acta Cryst.* C**57**, 1106–1108.
Boudjada, F., Meinnel, J., Cousson, A., Paulus, W., Mani, M. & Sanquer, M. (1999). *AIP Conf. Proc.* pp. 217–222.
Bruker (2006). *APEX2*, *SAINT* and *SADABS*. Bruker AXS Inc., Madison, Wisconsin, USA.
Burla, M. C., Caliandro, R., Camalli, M., Carrozzini, B., Cascarano, G. L., De Caro, L., Giacovazzo, C., Polidori, G. & Spagna, R. (2005). *J. Appl. Cryst.* **38**, 381–388.
Farrugia, L. J. (2012). *J. Appl. Cryst.* **45**, 849–854.
Groom, C. R., Bruno, I. J., Lightfoot, M. P. & Ward, S. C. (2016). *Acta Cryst.* B**72**, 171–179.
Hernandez, O., Cousson, A., Plazanet, M., Nierlich, M. & Meinnel, J. (2003). *Acta Cryst.* C**59**, o445–o450.
Macrae, C. F., Sovago, I., Cottrell, S. J., Galek, P. T. A., McCabe, P., Pidcock, E., Platings, M., Shields, G. P., Stevens, J. S., Towler, M. & Wood, P. A. (2020). *J. Appl. Cryst.* **53**, 226–235.
McKinnon, J. J., Jayatilaka, D. & Spackman, M. A. (2007). *Chem. Commun.* pp. 3814.
Medjroubi, M. L., Boudjada, A., Hamdouni, N., Jeannin, O. & Meinnel, J. (2017). *IUCrData*, **2**, x170672.
Medjroubi, M. L., Jeannin, O., Fourmigué, M., Boudjada, A. & Meinnel, J. (2016). *IUCrData*, **1**, x160621.
Sheldrick, G. M. (2015). *Acta Cryst.* C**71**, 3–8.
Spackman, M. A. & Jayatilaka, D. (2009). *CrystEngComm*, **11**, 19–32.
Tazi, M., Meinnel, J., Sanquer, M., Nusimovici, M., Tonnard, F. & Carrie, R. (1995). *Acta Cryst.* B**51**, 838–847.
Turner, M. J., McKinnon, J. J., Wolff, S. K., Grimwood, D. J., Spackman, P. R., Jayatilaka, D. & Spackman, M. A. (2017). *CrystalExplorer17. University of Western Australia.* http://hirshfeldsurface.net.

# supporting information

*Acta Cryst.* (2020). E**76**, 1391-1397 [https://doi.org/10.1107/S2056989020010270]

## Crystal structure and Hirshfeld surface analysis of 2,6-diiodo-4-nitrotoluene and 2,4,6-tribromotoluene

**Mohamed Larbi Medjroubi, Ali Boudjada, Noudjoud Hamdouni, Ouarda Brihi, Olivier Jeannin and Jean Meinnel**

### Computing details

For both structures, data collection: *APEX2* (Bruker, 2006); cell refinement: *SAINT* (Bruker, 2006); data reduction: *SAINT* (Bruker, 2006); program(s) used to solve structure: *SIR2004* (Burla *et al.*, 2005). Program(s) used to refine structure: *SHELXL97* (Sheldrick, 2015) for DINT; *SHELXL2018*/3 (Sheldrick, 2015) for TBT. For both structures, molecular graphics: *ORTEP-3 for Windows* (Farrugia, 2012) and *Mercury* (Macrae *et al.*, 2020); software used to prepare material for publication: *WinGX* publication routines (Farrugia, 2012).

### 2,6-Diiodo-4-nitrotoluene (DINT)

*Crystal data*

$C_7H_5I_2NO_2$
$M_r$ = 388.92
Monoclinic, $P2_1/c$
Hall symbol: -P 2ybc
$a$ = 4.3815 (2) Å
$b$ = 15.3348 (6) Å
$c$ = 14.5894 (6) Å
$\beta$ = 96.588 (1)°
$V$ = 973.78 (7) Å$^3$
$Z$ = 4
$F(000)$ = 704
$D_x$ = 2.653 Mg m$^{-3}$
Mo $K\alpha$ radiation, $\lambda$ = 0.71073 Å
Cell parameters from 3615 reflections
$\theta$ = 2.8–27.4°
$\mu$ = 6.42 mm$^{-1}$
$T$ = 150 K
Prism, colourless
0.29 × 0.13 × 0.06 mm

*Data collection*

Bruker APEXII diffractometer
CCD rotation images, thin slices scans
Absorption correction: multi-scan (SADABS; Bruker, 2006)
$T_{min}$ = 0.382, $T_{max}$ = 0.680
4104 measured reflections
2244 independent reflections
1850 reflections with $I > 2\sigma(I)$
$R_{int}$ = 0.022
$\theta_{max}$ = 27.5°, $\theta_{min}$ = 2.7°
$h$ = −5→5
$k$ = −19→19
$l$ = 0→18

*Refinement*

Refinement on $F^2$
Least-squares matrix: full
$R[F^2 > 2\sigma(F^2)]$ = 0.024
$wR(F^2)$ = 0.046
$S$ = 0.98
2244 reflections
110 parameters
0 restraints
Primary atom site location: structure-invariant direct methods
Secondary atom site location: difference Fourier map
Hydrogen site location: inferred from neighbouring sites

H-atom parameters constrained
$w = 1/[\sigma^2(F_o^2) + (0.0064P)^2]$
where $P = (F_o^2 + 2F_c^2)/3$

$(\Delta/\sigma)_{max} = 0.001$
$\Delta\rho_{max} = 0.65$ e Å$^{-3}$
$\Delta\rho_{min} = -0.55$ e Å$^{-3}$

*Fractional atomic coordinates and isotropic or equivalent isotropic displacement parameters (Å²)*

| | *x* | *y* | *z* | $U_{iso}$*/$U_{eq}$ |
|---|---|---|---|---|
| I2 | 0.49927 (5) | 0.16308 (2) | 0.43507 (2) | 0.02865 (8) |
| I1 | 0.61809 (6) | −0.09049 (2) | 0.11508 (2) | 0.03239 (8) |
| O2 | 1.0610 (7) | 0.31383 (17) | 0.16120 (19) | 0.0439 (7) |
| O1 | 1.2265 (6) | 0.21412 (17) | 0.07502 (18) | 0.0383 (6) |
| N1 | 1.0741 (6) | 0.2380 (2) | 0.1357 (2) | 0.0270 (7) |
| C4 | 0.9021 (7) | 0.1719 (2) | 0.1809 (2) | 0.0213 (7) |
| C5 | 0.7967 (7) | 0.1926 (2) | 0.2637 (2) | 0.0226 (7) |
| C7 | 0.4089 (8) | −0.0220 (2) | 0.3155 (3) | 0.0311 (8) |
| C3 | 0.8521 (7) | 0.0917 (2) | 0.1389 (2) | 0.0248 (8) |
| C6 | 0.6400 (7) | 0.1288 (2) | 0.3069 (2) | 0.0223 (7) |
| C1 | 0.5769 (7) | 0.0462 (2) | 0.2676 (2) | 0.0238 (8) |
| C2 | 0.6870 (7) | 0.0302 (2) | 0.1830 (2) | 0.0243 (8) |
| H5 | 0.830322 | 0.248772 | 0.290300 | 0.027* |
| H3 | 0.927896 | 0.078917 | 0.081954 | 0.030* |
| H7A | 0.556153 | −0.056139 | 0.356537 | 0.047* |
| H7B | 0.298926 | −0.060732 | 0.269445 | 0.047* |
| H7C | 0.261494 | 0.006076 | 0.351681 | 0.047* |

*Atomic displacement parameters (Å²)*

| | $U^{11}$ | $U^{22}$ | $U^{33}$ | $U^{12}$ | $U^{13}$ | $U^{23}$ |
|---|---|---|---|---|---|---|
| I2 | 0.02982 (13) | 0.03671 (15) | 0.02075 (13) | 0.00201 (11) | 0.00862 (10) | −0.00039 (10) |
| I1 | 0.03450 (14) | 0.02883 (14) | 0.03341 (16) | −0.00032 (11) | 0.00206 (11) | −0.00721 (11) |
| O2 | 0.0607 (19) | 0.0330 (15) | 0.0414 (18) | −0.0150 (14) | 0.0212 (15) | −0.0067 (13) |
| O1 | 0.0426 (16) | 0.0438 (16) | 0.0318 (16) | 0.0010 (13) | 0.0189 (13) | 0.0059 (13) |
| N1 | 0.0268 (15) | 0.0334 (17) | 0.0210 (16) | −0.0023 (14) | 0.0039 (13) | 0.0026 (14) |
| C4 | 0.0170 (16) | 0.0263 (18) | 0.0206 (18) | 0.0018 (14) | 0.0014 (13) | 0.0045 (14) |
| C5 | 0.0216 (17) | 0.0259 (18) | 0.0200 (18) | 0.0007 (14) | 0.0009 (14) | 0.0011 (15) |
| C7 | 0.0290 (19) | 0.030 (2) | 0.035 (2) | −0.0010 (17) | 0.0083 (16) | 0.0031 (17) |
| C3 | 0.0226 (17) | 0.0310 (19) | 0.0204 (19) | 0.0045 (15) | 0.0010 (14) | −0.0018 (15) |
| C6 | 0.0185 (16) | 0.0330 (19) | 0.0148 (18) | 0.0066 (15) | −0.0007 (14) | 0.0009 (15) |
| C1 | 0.0200 (16) | 0.0279 (19) | 0.0229 (19) | 0.0055 (15) | −0.0003 (14) | 0.0034 (15) |
| C2 | 0.0224 (17) | 0.0233 (18) | 0.026 (2) | 0.0011 (15) | −0.0015 (15) | −0.0029 (15) |

*Geometric parameters (Å, º)*

| | | | |
|---|---|---|---|
| I2—C6 | 2.101 (3) | C7—C1 | 1.497 (5) |
| I1—C2 | 2.105 (3) | C7—H7A | 0.9800 |
| O2—N1 | 1.224 (4) | C7—H7B | 0.9800 |
| O1—N1 | 1.224 (4) | C7—H7C | 0.9800 |
| N1—C4 | 1.464 (4) | C3—C2 | 1.389 (5) |

| | | | |
|---|---|---|---|
| C4—C5 | 1.378 (5) | C3—H3 | 0.9500 |
| C4—C3 | 1.381 (5) | C6—C1 | 1.404 (5) |
| C5—C6 | 1.388 (5) | C1—C2 | 1.398 (5) |
| C5—H5 | 0.9500 | | |

| | | | |
|---|---|---|---|
| O2—N1—O1 | 123.5 (3) | H7B—C7—H7C | 109.5 |
| O2—N1—C4 | 118.4 (3) | C4—C3—C2 | 117.6 (3) |
| O1—N1—C4 | 118.0 (3) | C4—C3—H3 | 121.2 |
| C5—C4—C3 | 122.8 (3) | C2—C3—H3 | 121.2 |
| C5—C4—N1 | 118.5 (3) | C5—C6—C1 | 122.3 (3) |
| C3—C4—N1 | 118.7 (3) | C5—C6—I2 | 116.1 (2) |
| C4—C5—C6 | 118.0 (3) | C1—C6—I2 | 121.7 (3) |
| C4—C5—H5 | 121.0 | C2—C1—C6 | 116.5 (3) |
| C6—C5—H5 | 121.0 | C2—C1—C7 | 121.8 (3) |
| C1—C7—H7A | 109.5 | C6—C1—C7 | 121.6 (3) |
| C1—C7—H7B | 109.5 | C3—C2—C1 | 122.7 (3) |
| H7A—C7—H7B | 109.5 | C3—C2—I1 | 115.7 (3) |
| C1—C7—H7C | 109.5 | C1—C2—I1 | 121.6 (3) |
| H7A—C7—H7C | 109.5 | | |

| | | | |
|---|---|---|---|
| O2—N1—C4—C5 | −15.8 (4) | C5—C6—C1—C2 | 1.5 (5) |
| O1—N1—C4—C5 | 163.4 (3) | I2—C6—C1—C2 | −178.8 (2) |
| O2—N1—C4—C3 | 164.2 (3) | C5—C6—C1—C7 | 179.7 (3) |
| O1—N1—C4—C3 | −16.7 (4) | I2—C6—C1—C7 | −0.6 (4) |
| C3—C4—C5—C6 | 1.5 (5) | C4—C3—C2—C1 | −1.2 (5) |
| N1—C4—C5—C6 | −178.6 (3) | C4—C3—C2—I1 | 179.8 (2) |
| C5—C4—C3—C2 | 0.3 (5) | C6—C1—C2—C3 | 0.3 (5) |
| N1—C4—C3—C2 | −179.7 (3) | C7—C1—C2—C3 | −177.8 (3) |
| C4—C5—C6—C1 | −2.4 (5) | C6—C1—C2—I1 | 179.2 (2) |
| C4—C5—C6—I2 | 177.9 (2) | C7—C1—C2—I1 | 1.1 (4) |

## 2,4,6-Tribromotoluene (TBT)

*Crystal data*

$C_7H_5Br_3$
$M_r$ = 328.84
Monoclinic, $P2_1/n$
$a$ = 14.3484 (11) Å
$b$ = 3.9955 (3) Å
$c$ = 15.6975 (12) Å
$\beta$ = 110.519 (2)°
$V$ = 842.83 (11) Å$^3$
$Z$ = 4

$F(000)$ = 608
$D_x$ = 2.592 Mg m$^{-3}$
Mo $K\alpha$ radiation, $\lambda$ = 0.71073 Å
Cell parameters from 2989 reflections
$\theta$ = 2.4–27.5°
$\mu$ = 14.28 mm$^{-1}$
$T$ = 150 K
Prism, colourless
0.34 × 0.21 × 0.12 mm

*Data collection*

Bruker APEXII diffractometer
CCD rotation images, thin slices scans
Absorption correction: multi-scan (SADABS; Bruker, 2006)

$T_{min}$ = 0.496, $T_{max}$ = 0.746
6197 measured reflections
1928 independent reflections
1657 reflections with $I > 2\sigma(I)$
$R_{int}$ = 0.027

$\theta_{max}$ = 27.5°, $\theta_{min}$ = 2.4°
$h$ = −18→18
$k$ = −4→5
$l$ = −18→20

*Refinement*

Refinement on $F^2$
Least-squares matrix: full
$R[F^2 > 2\sigma(F^2)]$ = 0.025
$wR(F^2)$ = 0.049
$S$ = 1.08
1928 reflections
93 parameters
0 restraints
Primary atom site location: structure-invariant direct methods
Secondary atom site location: difference Fourier map
Hydrogen site location: inferred from neighbouring sites
H-atom parameters constrained
$w = 1/[\sigma^2(F_o^2) + (0.0154P)^2 + 1.1776P]$ where $P = (F_o^2 + 2F_c^2)/3$
$(\Delta/\sigma)_{max}$ = 0.001
$\Delta\rho_{max}$ = 0.70 e Å$^{-3}$
$\Delta\rho_{min}$ = −0.68 e Å$^{-3}$
Extinction correction: SHELXL-2018/3 (Sheldrick 2015), $Fc^*=kFc[1+0.001xFc^2\lambda^3/\sin(2\theta)]^{-1/4}$
Extinction coefficient: 0.00060 (17)

*Special details*

**Geometry**. All esds (except the esd in the dihedral angle between two l.s. planes) are estimated using the full covariance matrix. The cell esds are taken into account individually in the estimation of esds in distances, angles and torsion angles; correlations between esds in cell parameters are only used when they are defined by crystal symmetry. An approximate (isotropic) treatment of cell esds is used for estimating esds involving l.s. planes.

*Fractional atomic coordinates and isotropic or equivalent isotropic displacement parameters (Å²)*

| | $x$ | $y$ | $z$ | $U_{iso}$*/$U_{eq}$ |
|---|---|---|---|---|
| Br1 | 0.68701 (2) | 1.18762 (9) | 0.84471 (2) | 0.02351 (10) |
| Br2 | 0.36077 (2) | 0.60522 (9) | 0.90955 (2) | 0.02044 (10) |
| Br3 | 0.35213 (2) | 0.68698 (9) | 0.55023 (2) | 0.02088 (10) |
| C1 | 0.5156 (2) | 0.9306 (8) | 0.7029 (2) | 0.0151 (7) |
| C2 | 0.5592 (2) | 0.9823 (8) | 0.7965 (2) | 0.0165 (7) |
| C3 | 0.5158 (2) | 0.8920 (8) | 0.8588 (2) | 0.0167 (7) |
| H3 | 0.548214 | 0.934507 | 0.921902 | 0.020* |
| C4 | 0.4234 (2) | 0.7369 (8) | 0.8266 (2) | 0.0154 (7) |
| C5 | 0.3755 (2) | 0.6790 (8) | 0.7351 (2) | 0.0148 (7) |
| H5 | 0.312062 | 0.574516 | 0.713540 | 0.018* |
| C6 | 0.4217 (2) | 0.7759 (8) | 0.6756 (2) | 0.0156 (7) |
| C7 | 0.5638 (2) | 1.0280 (9) | 0.6357 (2) | 0.0219 (8) |
| H7A | 0.576650 | 0.826805 | 0.605878 | 0.033* |
| H7B | 0.626764 | 1.142988 | 0.667500 | 0.033* |
| H7C | 0.519404 | 1.177907 | 0.589887 | 0.033* |

*Atomic displacement parameters (Å²)*

| | $U^{11}$ | $U^{22}$ | $U^{33}$ | $U^{12}$ | $U^{13}$ | $U^{23}$ |
|---|---|---|---|---|---|---|
| Br1 | 0.01425 (15) | 0.0243 (2) | 0.02664 (18) | −0.00447 (13) | 0.00050 (13) | 0.00205 (15) |
| Br2 | 0.02155 (16) | 0.0246 (2) | 0.01674 (16) | −0.00194 (14) | 0.00871 (12) | 0.00230 (14) |
| Br3 | 0.02070 (16) | 0.0273 (2) | 0.01272 (15) | −0.00059 (14) | 0.00346 (12) | −0.00326 (14) |
| C1 | 0.0149 (14) | 0.0130 (17) | 0.0176 (15) | 0.0034 (13) | 0.0058 (12) | 0.0028 (13) |
| C2 | 0.0139 (14) | 0.0131 (17) | 0.0191 (15) | −0.0009 (12) | 0.0016 (12) | 0.0024 (13) |
| C3 | 0.0176 (15) | 0.0133 (17) | 0.0146 (15) | 0.0003 (13) | −0.0002 (12) | −0.0026 (13) |

| | | | | | | |
|---|---|---|---|---|---|---|
| C4 | 0.0166 (14) | 0.0153 (18) | 0.0161 (15) | 0.0033 (13) | 0.0081 (12) | 0.0007 (13) |
| C5 | 0.0123 (14) | 0.0148 (17) | 0.0163 (15) | −0.0015 (12) | 0.0039 (12) | −0.0013 (13) |
| C6 | 0.0173 (14) | 0.0134 (17) | 0.0133 (14) | 0.0030 (13) | 0.0017 (12) | −0.0041 (13) |
| C7 | 0.0162 (15) | 0.029 (2) | 0.0213 (17) | 0.0023 (14) | 0.0074 (13) | 0.0042 (15) |

*Geometric parameters (Å, º)*

| | | | |
|---|---|---|---|
| Br1—C2 | 1.907 (3) | C3—H3 | 0.9500 |
| Br2—C4 | 1.898 (3) | C4—C5 | 1.377 (4) |
| Br3—C6 | 1.903 (3) | C5—C6 | 1.376 (5) |
| C1—C2 | 1.396 (4) | C5—H5 | 0.9500 |
| C1—C6 | 1.405 (4) | C7—H7A | 0.9800 |
| C1—C7 | 1.502 (4) | C7—H7B | 0.9800 |
| C2—C3 | 1.379 (5) | C7—H7C | 0.9800 |
| C3—C4 | 1.389 (4) | | |
| | | | |
| C2—C1—C6 | 114.5 (3) | C6—C5—C4 | 118.5 (3) |
| C2—C1—C7 | 123.6 (3) | C6—C5—H5 | 120.8 |
| C6—C1—C7 | 121.9 (3) | C4—C5—H5 | 120.7 |
| C3—C2—C1 | 124.1 (3) | C5—C6—C1 | 123.7 (3) |
| C3—C2—Br1 | 116.2 (2) | C5—C6—Br3 | 116.5 (2) |
| C1—C2—Br1 | 119.7 (2) | C1—C6—Br3 | 119.8 (2) |
| C2—C3—C4 | 118.0 (3) | C1—C7—H7A | 109.5 |
| C2—C3—H3 | 121.0 | C1—C7—H7B | 109.5 |
| C4—C3—H3 | 121.0 | H7A—C7—H7B | 109.5 |
| C5—C4—C3 | 121.2 (3) | C1—C7—H7C | 109.5 |
| C5—C4—Br2 | 119.1 (2) | H7A—C7—H7C | 109.5 |
| C3—C4—Br2 | 119.7 (2) | H7B—C7—H7C | 109.5 |
| | | | |
| C6—C1—C2—C3 | 0.0 (5) | C3—C4—C5—C6 | 0.5 (5) |
| C7—C1—C2—C3 | −179.6 (3) | Br2—C4—C5—C6 | 179.9 (2) |
| C6—C1—C2—Br1 | 179.7 (2) | C4—C5—C6—C1 | 0.2 (5) |
| C7—C1—C2—Br1 | 0.1 (5) | C4—C5—C6—Br3 | 179.7 (2) |
| C1—C2—C3—C4 | 0.7 (5) | C2—C1—C6—C5 | −0.5 (5) |
| Br1—C2—C3—C4 | −179.0 (2) | C7—C1—C6—C5 | 179.2 (3) |
| C2—C3—C4—C5 | −0.9 (5) | C2—C1—C6—Br3 | −179.9 (2) |
| C2—C3—C4—Br2 | 179.7 (2) | C7—C1—C6—Br3 | −0.3 (4) |